Open access • Journal Article • DOI:10.1021/ACS.JPCC.7B06890

Properties of Functionalized Carbon Nanotubes and Their Interaction with a Metallic Substrate Investigated by Scanning Tunneling Microscopy — Source link

Van Dong Pham, Vincent Repain, Cyril Chacon, Amandine Bellec ...+9 more authors

Institutions: Paris Diderot University, Université Paris-Saclay, Shinshu University, Pennsylvania State University ...+1 more institutions

Published on: 23 Oct 2017 - Journal of Physical Chemistry C (American Chemical Society)

Topics: Optical properties of carbon nanotubes, Mechanical properties of carbon nanotubes, Selective chemistry of single-walled nanotubes, Carbon nanotube and Scanning tunneling microscope

Properties of Functionalized Carbon Nanotubes and Their Interaction with a Metallic Substrate Investigated by Scanning Tunneling Microscopy

Van Dong Pham; Repain, Vincent; Chacon, Cyril; Bellec, Amandine; Girard, Yann; Rousset, Sylvie; Campidelli, Stephane; Lauret, Jean-Sebastien; Voisin, Christophe; Terrones, Mauricio

Published in:
Journal of Physical Chemistry C

DOI:
10.1021/acs.jpcc.7b06890

Publication date:
2017

THE JOURNAL OF PHYSICAL CHEMISTRY C

Article

Cite This: J. Phys. Chem. C 2017, 121, 24264-24271

pubs.acs.org/JPCC

Properties of Functionalized Carbon Nanotubes and Their Interaction with a Metallic Substrate Investigated by Scanning Tunneling Microscopy

Van Dong Pham,[†] Vincent Repain,[†] Cyril Chacon,[†] Amandine Bellec,[†] Yann Girard,[†] Sylvie Rousset,[†] Stephane Campidelli,[‡] Jean-Sébastien Lauret,[§] Christophe Voisin,[∥] Mauricio Terrones,[⊥,#] Maria Cristina dos Santos,[¶] and Jérôme Lagoute*,[†]

[†]Laboratoire Matériaux et Phénomènes Quantiques, Université Paris Diderot, Sorbonne Paris Cité, CNRS, UMR 7162, 75013 Paris, France

[‡]LICSEN, NIMBE, CEA, CNRS, Université Paris-Saclay, CEA-Saclay, Gif-sur-Yvette 91191 Cedex, France

[§]Laboratoire Aimé Cotton, CNRS, Université Paris-Sud, ENS Cachan, Université Paris-Saclay, Orsay 91405 Cedex, France

[∥]Laboratoire Pierre Aigrain, Ecole Normale Supérieure, CNRS, UPMC, Université Paris Diderot, Paris, France

[⊥]Department of Physics and Center for 2-Dimensional and Layered Materials, The Pennsylvania State University, University Park, Pennsylvania 16802, United States

[#]Institute of Carbon Science and Technology, Shinshu University, 4-17-1 Wakasato, Nagano City 380-8553, Japan

[¶]Zernike Institute for Advanced Materials, University of Groningen Nijenborgh 4, Groningen 9747 AG, The Netherlands

Supporting Information

ABSTRACT: Noncovalent functionalization of carbon nanotubes (CNTs) allows the combination of the remarkable physical properties of these one-dimensional systems with the properties of the functional molecules and, at the same time, modifies the physicochemical properties of nanotubes for specific applications. The use of functionalized carbon nanotubes in electronics often requires the deposition of the nanotubes on a substrate, and eventually an annealing step, which can modify their properties due to molecule−surface interactions. Using scanning tunneling microscopy/spectroscopy (STM/STS) and classical molecular dynamics (MD) simulations we studied the physical properties of carbon nanotubes functionalized with porphyrin derivatives and discuss the effect of physisorption and sample annealing on the nanotube surface. The results reveal that the functionalized parts exhibit nonperiodic structure with a significant modification of the local density of states. The coverage degree can be estimated from STM images. When the sample is annealed, STM data clearly show an unwrapping of the functionalizing species leading to a lowering of the coverage degree. In addition, periodic structures were observed that correspond to the surfactants originally present in the CNT sample, revealing that the surfactants are still present in such functionalized nanotubes. These results provide information on the structure and properties of polymer-functionalized nanotubes and the effect of substrate interaction and sample annealing that can markedly modify the structure and properties of the functionalized nanotubes.

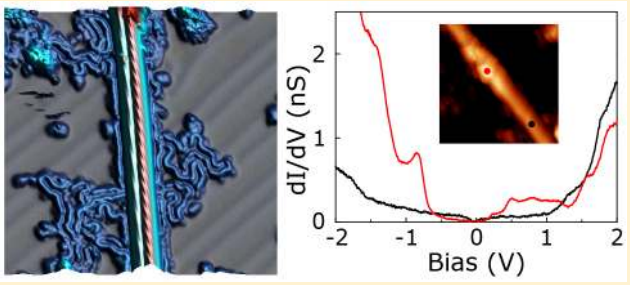

INTRODUCTION

Due to their remarkable physical and electronic properties, single-walled carbon nanotubes (CNTs) offer numerous possibilities to be integrated into electronic devices[1−13] or biosensors.[14−16] Furthermore, functionalization of CNTs has initially been recognized as an important prerequisite for improving the solubility of CNTs in the liquid phase[17] and allows us to combine novel properties and fabricate functional materials.[18−28] However, the integration of functionalized CNTs in devices often requires one to deposit them on a supporting substrate. This process may unexpectedly affect the intrinsic properties of the functionalized nanotubes because the tubes can undergo an electronic coupling with the substrate, and their electrostatic charges can vary significantly, thus altering the electrical conductance[29,30] and the electronic/optical properties of the device.[31] When fabricating sensors using chemically functionalized nanotubes connected to gold electrodes, thermal annealing up to 300 °C is often used to improve the contact between the nanotubes and the electrodes.[32−35] Since this annealing procedure may modify the

Received: July 13, 2017
Revised: October 7, 2017
Published: October 9, 2017

DOI: 10.1021/acs.jpcc.7b06890
J. Phys. Chem. C 2017, 121, 24264−24271

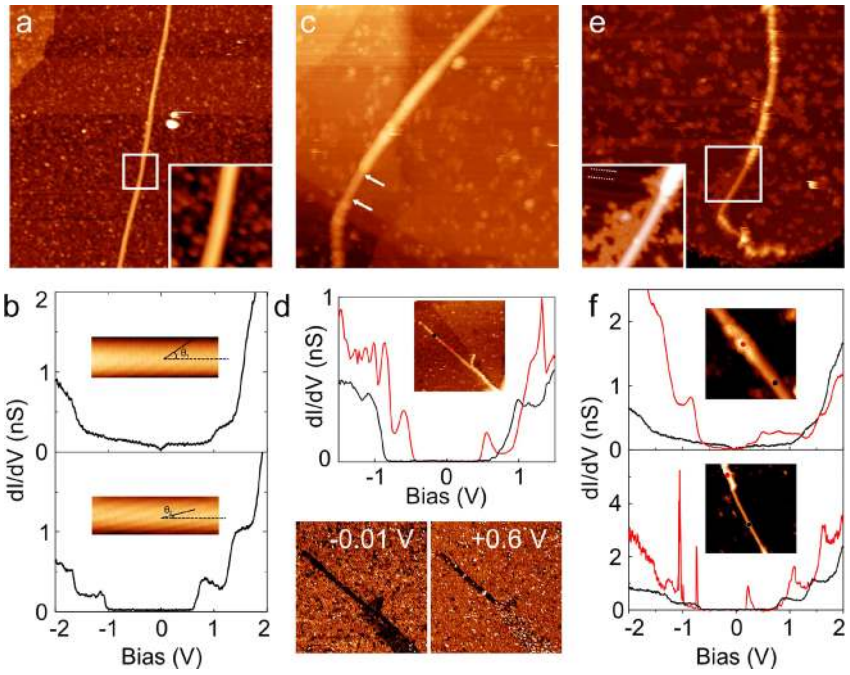

Figure 1. (a) STM image (150 × 150 nm^2) of a pristine nanotube on Au(111) after annealing at 430 K. The inset corresponds to the area marked by a square in the image. (b) *dI/dV* spectra on a metallic (top) and a semiconducting (bottom) pristine nanotube on the same sample as the one used in (a). The insets are topographic images of the tubes (image size 2 × 6 nm^2). (c) STM image (150 × 150 nm^2) of a functionalized nanotube on Au(111) without annealing. The part of the tube located between the two arrows is not functionalized. (d) Top: *dI/dV* spectra measured on the same sample as in (c) at the positions marked by the red and black dots in the topographic image reported in the inset. Bottom: Conductance maps close to the Fermi level (left) and at 0.6 V (right) measured on the same area as the topographic image in the inset. (e) STM image (150 × 150 nm^2) and spectroscopy of functionalized nanotubes on Au(111) after annealing at 380 K. The inset corresponds to the area marked by a square in the image. The dotted lines in the inset mark the Au(111) reconstruction lines. (f) *dI/dV* spectra on a metallic (top) and a semiconducting (bottom) functionalized nanotube on the same sample as the one used in (e). The insets show the topographies of both nanotubes and the locations where the spectra were measured (image size: 22 × 22 nm^2 (top), 60 × 60 nm^2 (bottom)).

surface of carbon nanotubes, it is important to clarify, at the molecular level, the functionalities present on the tubes. Therefore, it is necessary to perform molecular scale imaging of functionalized nanotubes and elucidate the structure of the organic layer interacting with the nanotube. Transmission electron microscopy (TEM)[36−38] has revealed the structures of some organic layers deposited on the CNT sidewalls. However, this technique does not allow us to visualize nanotubes in contact with a metallic electrode. Scanning tunneling microscopy and spectroscopy (STM/STS) allow atomic-scale imaging and electronic measurements of CNTs in contact with a metal. To date, many works have been reported on the STM characterization of CNTs functionalized with molecules, e.g., DNA wrapped on CNTs,[39] streptavidin,[40] nucleophile,[41] and aliphatic chains.[42] A spatial mapping of the electronic states has also been used to investigate local functionalization and doping.[43] However, in functionalized nanotubes, it is still challenging to visualize in detail the functional molecules, especially the electronic modification caused by the functionalization. Here, we investigate CNTs functionalized with a porphyrin polymer. The interaction of CNTs with porphyrin molecules is the subject of an intense research activity[44] and allows an efficient energy transfer under light excitation.[19] Previous work using global characterization techniques has shown that CNTs can be functionalized by porphyrins using the micelle swelling method[45−47] or by a porphyrin polymer.[38] However, a local investigation is needed in order to obtain information on the structure of the polymer, the coverage amount, the electronic properties of the funtionalized tube, and the role of surfactants, which are crucial parameters for applications based on such CNTs. Here, we study the structure and electronic properties of CNTs functionalized with a polymer of porphyrin. Nonperiodic structures are found that are related to the polymer functionalization. Periodic structures were also observed, revealing the presence of surfactants on the functionalized nanotubes. We measure the coverage degree from the STM images, which is an important quantity for applications using functionalized nanotubes.[48] After annealing, we show that the covering amount is reduced, and an unwrapping of the functionalization material is observed.

EXPERIMENTAL AND THEORETICAL METHODS

A detailed description of the preparation of dispersions containing CNTs wrapped by porphyrin polymers has been published elsewhere.[38] We used the same tubes in the present study. Briefly, 150 μL of a solution of tetrathioacetyl porphyrin (at 1 mg/mL in CH_2Cl_2) was added to a solution of laser ablation single-walled CNTs in 2 wt % SDS (5 mL). The mixture was sonicated for 30 min at the maximum power of a sonic bath (2.5 L Elmasonic T490DH bath 130 W, 40 kHz) to make CH_2Cl_2 (and consequentially the porphyrin derivatives) penetrate the micelles and then gently sonicated (power 40% of the sonic bath) for 2 h to remove CH_2Cl_2. Then, hydroxylamine 50 wt % in water (100 μL) and triethylamine (100 μL) were sequentially added. The reaction mixture was stirred at room temperature for 2 h and then placed under an O_2 atmosphere for 14 h. The solution was filtrated through polytetrafluoroethylene (PTFE) membranes (0.2 μm) and

DOI: 10.1021/acs.jpcc.7b06890
J. Phys. Chem. C 2017, 121, 24264−24271

washed sequentially with a mixture of H_2O/MeOH (30 mL, 1:1, v/v), tetrahydrofuran (THF) (30 mL), acetone (30 mL), *N*-methyl-pyrrolidone (NMP) (30 mL), and CH_2Cl_2 (30 mL) in order to remove the surfactant, the excess of reagents, and the unbound porphyrins. The buckypapers were briefly immersed into dry NMP (6 mL) under intense sonication and then gently sonicated for 10 min to give perfectly stable solutions.

The deposition of functionalized CNTs was prepared by dispersing the nanotube in the NMP solution using an ultrasonic sonicator with a tip in the solution in 30 s, then dropping the freshly sonicated solution onto a clean Au(111)/mica substrate. The surface was left in 15 min for the binding of functionalized CNTs on the surface, followed by cleaning with ethanol solution (6 mL) in order to remove the unbound nanotubes and NMP solvent. All STM measurements were performed using low-temperature STM equipment (Omicron) working at 4.6 K at a pressure lower than 1×10^{-10} mbar. The dI/dV spectra were acquired using a lock-in detector at a frequency of ca. 670 Hz and a modulation amplitude of 35 mV. The measurements were performed using an electrochemically etched tungsten tip. The clean Au(111)/mica substrate was prepared by several cycles of sputtering with Ar^+ at 900 eV followed by annealing at 600 K under UHV.

Carbon nanotubes interacting with tetrathioacetyl porphyrins (TTPs) in water−SDS environment were studied by classical molecular dynamics (MD). A box of dimensions (44.7 × 44.7 × 39.6 Å) containing a (6,5) nanotube in its center was filled with 6 TTP molecules, 8 dissociated SDS (DS^- + Na^+) amphiphiles, and 3243 water molecules. Periodic boundary conditions were applied, and the NPT ensemble (constant number of particles, constant pressure, constant temperature) was chosen for these simulations, adopting ambient conditions (T = 298 K and p = 0 GPa). Temperature and pressure controls were made by a Nosé−Hoover−Langevin thermostat and Berendsen barostat, respectively. The integration time step was 1 fs, and after equilibration of the simulation box, the calculations run for 500 ps. The force field COMPASS[49] was used. Partial charges on atoms were chosen as those internally stored in the force field, unless for SDS molecules, for which a partial charge of +1 was assigned to sodium ions and the −1 charge of dodecyl sulfate was rearranged through the Rappé−Goddard charge equilibration scheme. Calculations were carried out within the software Materials Studio 7.0.[50] The last simulation frame was used to build the porphyrin polymer. A superstructure was built using three repetitions of the simulation box along the nanotube axis. Following the experimental procedure, in which a reagent was added to bind the porphyrins through S−S bonds from the thiol ends, the binding of porphyrins was made by connecting sulfur atoms from thiol groups that were close enough to allow a S−S bond (and eliminating the pair of hydrogens). A similar procedure was adopted using the nanotubes (12,10) and (15,0), whose diameters are closer to the average diameter of laser ablation nanotubes. The number of porphyrins and SDS molecules was the same as for the nanotube (6,5), but the number of water molecules and the box dimensions were adjusted to accommodate the larger tubes.

RESULTS AND DISCUSSION

We start with the properties of pristine single-walled carbon nanotubes (obtained by the laser ablation method) deposited on Au(111) as a control experiment (see Methods). Figure 1a shows an STM image of a bare CNT without porphyrin molecules adsorbed on a Au(111) substrate. The tube appears clean, indicating that no contaminant is attached to the tube sidewall (see inset for a zoomed area). In order to access the electronic properties of carbon nanotubes, we carried out dI/dV spectroscopy which is proportional to the local density of states (LDOS). Figure 1b shows two representative dI/dV spectra that are fingerprints of a metallic tube (with a chiral angle of θ_1 = 30° obtained from an atomically resolved tube, see inset) and a semiconducting tube (chiral angle of θ_2 = 19.5°, see inset) with a gap of 1.5 eV between the first two van Hove singularities.[51,52] The mean value of the apparent diameter measured from the width of 30 CNTs in the STM images is 2.6 nm, which is larger than the known mean diameter of 1.2−1.3 nm, characteristic of the tubes we used here. The significantly large value found from the STM images is due to a convolution of the nanotube topography given by the shape of the STM tip.[53] The images and spectra are characteristic of pristine nanotubes, which confirms that the sample preparation does not produce contamination on the nanotubes.

We turn now to the case of CNTs functionalized by a porphyrin polymer which have been prepared using the micelle swelling technique described previously[38] (see Methods for details). We checked the functionalization of the CNTs by absorption spectroscopy, indicating characteristic features of both nanotubes and porphyrin molecules (see Supporting Information Figure S1). We also performed atomic force microscopy and scanning electron microscopy measurements that reveal the presence of the functionalizing material polymer (see Supporting Information Figure S2).

Figure 1c shows a representative STM image of a functionalized CNT deposited on Au(111). The typical apparent diameter in the STM images of this tube is 7 nm, which is larger than the mean value (2.6 nm) of bare CNTs measured on the first sample. Moreover, several protrusions can be seen on the nanotube. One part of the tube has a lower diameter, and no protrusion is observed; this part is identified as nonfunctionalized. This indicates that the molecules have been successfully attached to the tube sidewall and that the physisorbed tube is not fully covered. We have measured 46 tubes with a total length of 16 μm, and on each tube we measured the total length of the tube and the length of the tube that is covered. By taking the ratio of the total covered length and the total length measured on all the tubes, we estimated a coverage degree of 72%. This value can be taken as a lower limit of coverage degree since the interaction with the surface may eventually remove some functionalizing species and reduce the coverage degree as will be discussed below. In order to access to the electronic properties of the functionalized tubes, we performed dI/dV spectroscopy. Figure 1d shows two dI/dV spectra taken from different locations along the tubes that are shown in the inset. The black curve exhibits an electronic DOS with a gap of 1.8 eV that is taken from a part that is representative of most of the tube length. In contrast, the red curve taken from a specific location of the tube shows resonant states at −0.6 V and at +0.6 V. The latter clearly appears as a bright spot in the dI/dV map measured at 0.6 V reported in Figure 1d. The dI/dV map measured at −0.01 V shows that there is no state around the Fermi level and that all the tubes exhibit a semiconducting characteristic. The spectra taken on these functionalized tubes with this sample preparation procedure therefore exhibit complex spectroscopic features.

DOI: 10.1021/acs.jpcc.7b06890
J. Phys. Chem. C 2017, 121, 24264−24271

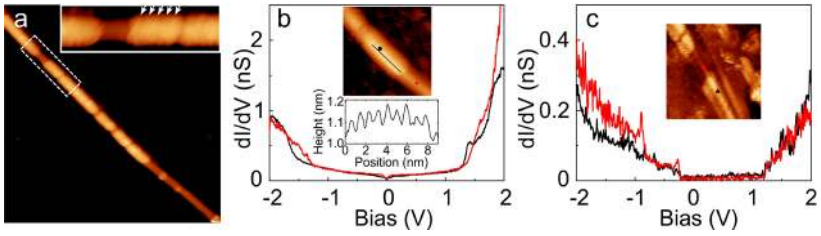

Figure 2. (a) STM images of functionalized nanotubes after deposition on Au(111) and annealing to 380 K. On this nanotube a pattern with a period of 0.8 nm is clearly visible. Image size: 51 × 51 nm^2. The inset corresponds to the rectangle drawn in the image. The arrows in the inset are spaced by 0.8 nm and mark the periodic structure. (b) *dI*/*dV* spectra measured above the metallic nanotubes shown in the inset (image size 20 × 20 nm^2) on the periodic structure (black) and on the pristine part (red). The linescan in the inset was measured along the line drawn in the image. (c) *dI*/*dV* spectra measured above the semiconducting nanotube shown in the inset (image size 20 × 20 nm^2) on the periodic structure (black) and on the pristine part (red).

As can be seen in the STM images (see Figure 1c), numerous particles are present on the Au surface, making STM investigations challenging. Therefore, in order to remove possible adsorbates from the Au(111) area, we further treated the sample by annealing at 380 K in ultrahigh vacuum (UHV). Figure 1e shows a typical STM image of a functionalized carbon nanotube after annealing the sample. Accordingly, we observe a functionalized CNT laying on the cleaner Au(111) surface. It can be clearly seen that the tube is partly decorated with molecules (bright lumps in the upper part) and partly uncovered (bottom part and inset). Surprisingly, around this uncovered location, we can clearly observe ribbons laying on the nearby gold substrate (see inset and below). To compare with the previous raw sample, we have measured 15 nanotubes with a total length of 2.5 μm and found a surface coverage of 22%. This suggests that the UHV annealing procedure removes the covering layer. This could be due to a thermally activated polymer removal without chemical degradation or involving the breaking or the dithiol groups that bridge the porphyrin molecules. Interestingly, we were able to see the herringbone reconstruction of Au(111) indicating that the surface is considerably cleaner. In order to understand the electronic properties of these tubes, we recorded *dI*/*dV* spectra above the lumpy areas on the tubes. Figure 1f (upper) reveals the *dI*/*dV* spectra of a metallic tube measured on the clean section (black curve) and on the covered part that appears rough in the STM image (red curve). The spectrum measured above the protrusion appears with a peak centered at −0.8 V and a broad hump ranging from +0.5 V to +1.4 V (black curve). Similar structures (i.e., rough tube surface and localized electronic states) are also observed on semiconducting tubes as displayed in Figure 1f (bottom). Therefore, the functionalization of the CNTs by a porphyrin polymer leads to the formation of localized electronic states on disordered structures covering the tube sidewall. However, it has to be noticed that periodic structures can also be found on the functionalized nanotubes as we describe in the following.

Figure 2 shows high-resolution STM images of different metallic and semiconducting tubes with a characteristic periodic pattern on their surface. These tubes are covered by molecules that form a wrapping structure with a periodicity of 0.8 nm around the tubes and an apparent height of 0.5 nm on the tube surface. However, there is no indication of the porphyrin molecular structure as observed previously on graphene[54] or on highly oriented pyrolytic graphite.[55] As described in the Methods section, the attachment of porphyrin molecules onto CNTs was obtained through the micelle swelling technique. The source of carbon nanotubes of our samples is a dispersion in sodium dodecyl sulfate (SDS) solutions. Although the final material has been filtered and washed to remove unreacted porphyrins, surfactants, and other reagents, it is clear from the STM images that the structures seen could be attributed to arrays of SDS molecules covering the nanotubes. Moreover, it is possible that part of the SDS suspended nanotubes did not interact with porphyrins and are present in the filtered material; hence SDS molecules remained in the sample. Another reason for the presence of SDS could be that the surfactant is trapped in the porphyrin polymer during its formation. Indeed, the polymer forms an amorphous organic layer around the nanotubes,[38] and the empty space can be filled by the remaining surfactant molecules. To avoid this process, a solution could be to have less flexibility in the polymer, for example, by removing the ethylene chains between the phenyl groups of the porphyrins and the thiol groups. The molecular dynamics simulation results, as described below, indicate that SDS molecules attach to porphyrins and are part of the supramolecular structures wrapping CNTs. Thus, we attribute the periodic pattern to SDS molecules adsorbed on the tube sidewalls.

Figure 2b,c shows *dI*/*dV* spectra taken on covered (black curves) and uncovered (red curves) parts on metallic and semiconducting tubes. These spectra measured above the SDS molecules do not show any significant variation in the electronic structures of CNTs as measured on disordered structures (Figure 1f).

As mentioned above, ribbons can also be observed on Au(111) around uncovered parts of CNTs (Figure 1e). In order to gain insight into these structures, we recorded STM images at higher resolution. Figure 3a shows two functionalized tubes appearing with clean sidewalls but surrounded by a bundle of ribbons laying on the Au substrate. Such ribbons have been observed several times only around uncovered parts. Therefore, we attribute these ribbons to molecular structures that have been detached during the annealing process. We further investigated the electronic structure of these chain structures by *dI*/*dV* spectroscopy. Figure 3b (blue curve) shows a *dI*/*dV* spectrum measured on the chain-like structures which reveals no specific feature. Note that the *dI*/*dV* measured on clean Au(111) shows the onset of the Shockley surface state at −0.5 eV which indicates that the STM tip is well calibrated for spectroscopy measurement. We also noted the semiconducting and metallic properties of two different tubes shown in the image. We rule out that the ribbons are porphyrins because they should exhibit HOMO and LUMO resonances in the *dI*/*dV* spectrum.[54,56,57] Therefore, we attribute the ribbons to SDS molecules.

DOI: 10.1021/acs.jpcc.7b06890
J. Phys. Chem. C 2017, 121, 24264−24271

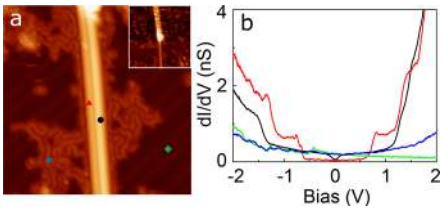

Figure 3. (a) STM image (35 × 35 nm^2, at −1 V, 550 pA) of a semiconducting (left) and a metallic (right) functionalized carbon nanotubes after deposition on Au(111) and annealing to 380 K. The inset shows a larger-scale image of the same tubes (100 × 100 nm^2, at −1 V, 250 pA). (b) Spectroscopy measured above the semiconducting nanotube (red) the metallic nanotube (black) and the unwrapped species (blue) at the positions indicated by the marks in (a). The reference spectrum (green) taken on the Au(111) terrace exhibits the expected Shockley state around −0.5 V.

The supramolecular structure of porphyrins and SDS wrapping a carbon nanotube in water was studied by classical molecular dynamics (MD). Figures 4a,b depict the simulation boxes at the end of the MD simulation (water molecules were omitted for clarity) for a semiconducting nanotube, (6,5), and a metallic nanotube, (15,0), whose diameters are, respectively, 0.74 and 1.17 nm. The number of organic molecules is the same in both simulation boxes, in order to represent the same concentration since the boxes were built to provide approximately the same volume outside the nanotubes. Sodium ions, the purple spheres in these figures, are trapped in the center of the macrocycles. SDS molecules are found on the nanotube surface and are part of the wrapping structure. According to recent studies of SDS wrapped nanotubes,[58] this surfactant is strongly bound to the nanotube surface, and it is thus expected to compete with the prophyrin adhesion at the nanotube walls. Moreover, in order to keep the charge neutrality, the organic anion should adhere to the porphyrins trapping a sodium ion.

The porphyrin polymer was constructed by binding sulfur atoms of neighboring molecules, as described in the Methods section. The porphyrins have four binding sites, resulting in a multiconnected polymer structure, as depicted in Figure 5. This figure also shows the molecular surfaces of polymer-wrapped nanotubes (6,5) and (15,0), obtained by the rolling sphere (radius 3 Å) method, also known as the Connolly surface. The shapes associated with the porphyrin macrocycle are easily distinguishable in the molecular surfaces, although there are no periodic features in these images. In order to account for the periodic striations seen in STM images shown in Figure 3, we assume that they correspond to SDS covering the nanotube walls. The structure of SDS-wrapped nanotubes in water was investigated by transmission electron microscopy (TEM)[59] in which striations were present and identified as micelles in the form of half cylinders. The shape and dimensions of these striations do not correspond to the images obtained by STM in the present work. The period of 0.8 nm and the thickness of 0.5 nm measured from the high-resolution STM images should be produced by a much simpler structure, such as that obtained by SDS molecules lying over the nanotube wall with the long molecular axis along the nanotube surface.

Several alkanes as well as cationic and anionic surfactants adsorbed on graphite have been studied and described as compact layers where the molecules form a lamellar structure.[60−66] Two geometries of the molecules with respect to the graphite surface have been observed, in which the plane that contains the carbon atoms is either parallel (face-on) or perpendicular (edge-on) to the graphite surface. The geometry of a face-on SDS layer was optimized on a (12,10) CNT, which is a semiconducting nanotube with a diameter that is in the range of the diameter of the nanotubes used in the experiment. The optimization leads to a periodic structure with an intermolecular distance of 0.45 nm, which agrees with the period of lamellar phases of alkanes and surfactants on graphite but is nearly half the experimentally measured period of the striations seen in Figure 2. We then built and optimized an alternating structure with face-on/edge-on arrangement of SDS molecules, as depicted in Figure 6. Compared to the all face-on array, the alternating array is more compact. The average distance between face-on SDS molecules is 0.86 nm, a value which is in agreement with the periodic structure observed by

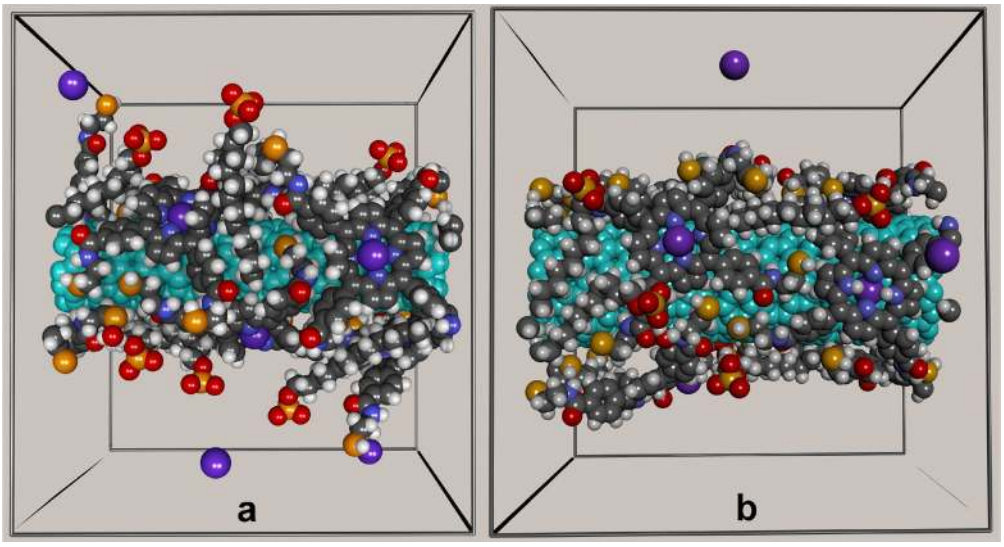

Figure 4. Snapshot of the MD simulation box: carbon nanotube surrounded by porphyrins and SDS molecules, tubes (a) (6,5) and (b) (15,0) (water molecules are not shown). Color scheme: the carbon nanotube is represented by cyan spheres; for the other structures, the spheres are gray for carbon, red for oxygen, white for hydrogen, blue for nitrogen, yellow for sulfur, and purple for sodium.

DOI: 10.1021/acs.jpcc.7b06890
J. Phys. Chem. C 2017, 121, 24264−24271

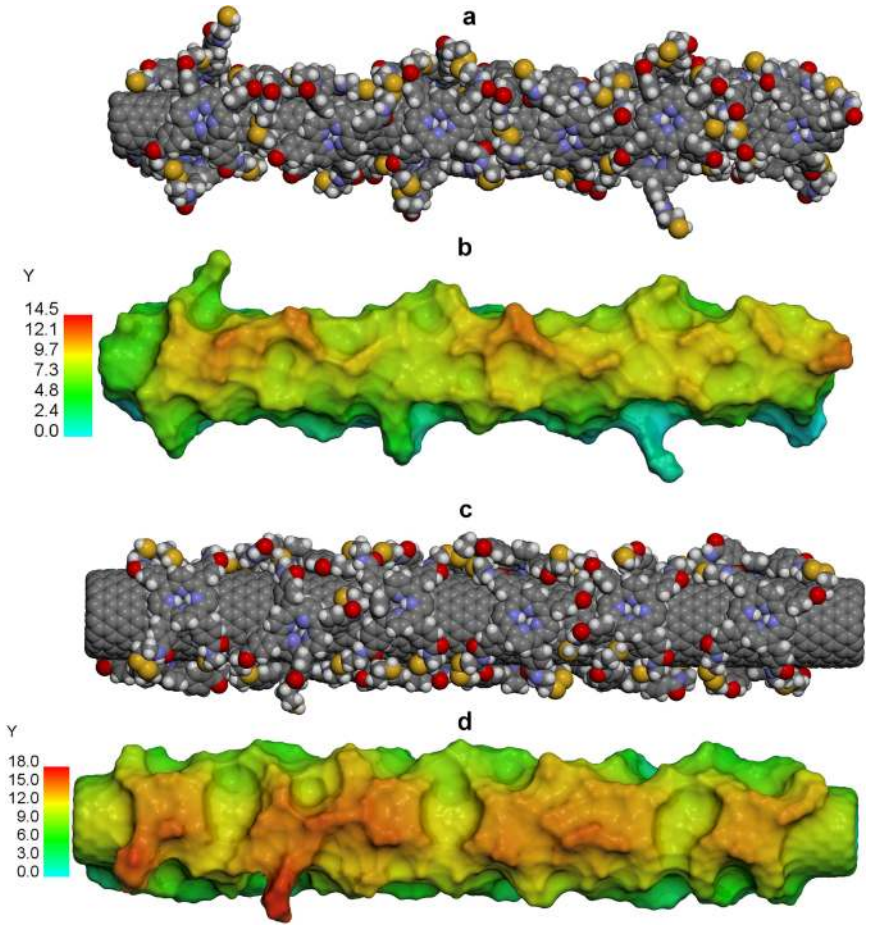

Figure 5. Structure and molecular surface of porphyrin polymer wrapping carbon nanotubes: (a) and (b) for nanotube (6,5) and (c) and (d) for the nanotube (15,0). Color scheme: gray for carbon, red for oxygen, white for hydrogen, blue for nitrogen, and yellow for sulfur. The surfaces are colored according to height; in the scale bar, given in Å, the *Y* axis is normal to the plane of the figure.

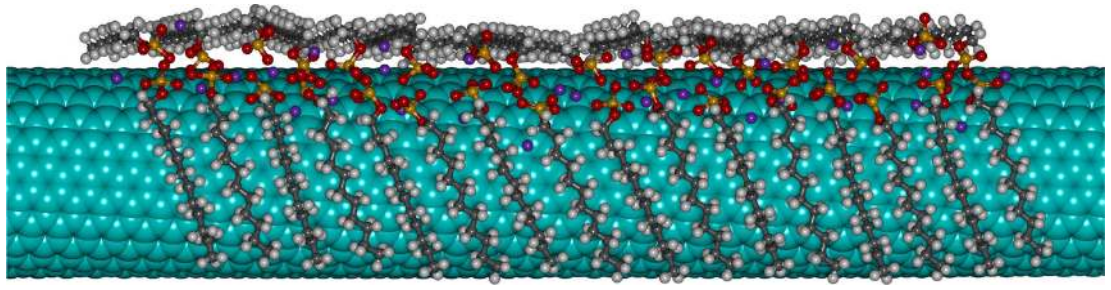

Figure 6. Structure of a (12,10) nanotube covered with SDS molecules. Color scheme: the nanotube is represented by light blue overlapping spheres and the surfactant molecules by ball-and-stick models with gray for carbon, red for oxygen, white for hydrogen, purple for sodium ions, and yellow for sulfur. Note the alternating face-on/edge-on structure of the SDS array.

STM. The absence of water in the samples prepared for STM and the in vacuo conditions of the measurements could be responsible for the growing of this thin and ordered SDS structure on the nanotube walls, seen here for the first time. Finally, a simulation was performed for the (6,5) nanotube wrapped with the porphyrin polymer and SDS molecules deposited on a gold slab, at room temperature and open boundary conditions, using the force field described in the Methods section. The nanotube slides on the gold surface, leaving the organic covering behind due to a stronger C−Au van der Waals interaction (Supplementary Video). This agrees with the fact that, after the thermal treatment of the samples, the nanotubes deposited on gold are seen mostly uncovered.

CONCLUSIONS

In summary, we have investigated the properties of carbon nanotubes functionalized with a porphyrin polymer and deposited on a metallic substrate. We have shown that the interaction between the nanotubes and the surface, especially when an annealing step is performed, can degrade the stability of functional groups. We evidenced a coverage degree of 72%, for a sample prepared at room temperature, that reduces to 22% after annealing the sample at 380 K. In particular, annealing leads to unwrapping of nanotubes. Our investigation has also revealed a very specific organization of SDS arranged with alternating orientations on the tube sidewalls and a lift off

DOI: 10.1021/acs.jpcc.7b06890
J. Phys. Chem. C 2017, 121, 24264−24271

of SDS induced by annealing. These results indicate that surface functionalization of nanotubes when constructing electronic devices has to be performed with care since tube surfaces could exhibit different electronic properties that could affect device performance.

■ ASSOCIATED CONTENT

Supporting Information

The Supporting Information is available free of charge on the ACS Publications website at DOI: 10.1021/acs.jpcc.7b06890.

Optical absorption spectroscopy of functionalized nanotubes (PDF)

Trajectory from a molecular dynamics simulation (NVT) with open boundary conditions and room temperature showing a (6,5) nanotube wrapped by a porphyrin polymer and SDS molecules on a gold slab (AVI)

■ AUTHOR INFORMATION

Corresponding Author

*E-mail: jerome.lagoute@univ-paris-diderot.fr.

ORCID

Stephane Campidelli: 0000-0001-6060-4891

Jean-Sébastien Lauret: 0000-0003-1309-4977

Christophe Voisin: 0000-0003-3175-9311

Jérôme Lagoute: 0000-0002-0568-6991

Notes

The authors declare no competing financial interest.

■ ACKNOWLEDGMENTS

MCS acknowledges the Research Computing and Cyberinfrastructure unit of Information Technology Services at Penn State University for providing access to the Materials Studio package and the financial support from the Brazilian Agency FAPESP (Fundação de Amparo à Pesquisa do Estado de São Paulo). ANR (Agence Nationale de la Recherche) and CGI/PIA (Commissariat Général à l'Investissement/Programme d'Investissement d'Avenir) ANR-11-IDEX-0005-02 are gratefully acknowledged for their financial support of this work through the Labex SEAM (Science and Engineering for Advanced Materials and devices) ANR 11 LABX 086.

■ REFERENCES

(1) Jiang, M.; Kumamoto, Y.; Ishii, A.; Yoshida, M.; Shimada, T.; Kato, Y. K. Gate-Controlled Generation of Optical Pulse Trains Using Individual Carbon Nanotubes. *Nat. Commun.* **2015**, *6*, 6335.

(2) Engel, M.; Steiner, M.; Seo, J.-W. T.; Hersam, M. C.; Avouris, P. Hot Spot Dynamics in Carbon Nanotube Array Devices. *Nano Lett.* **2015**, *15*, 2127−2131.

(3) Ranjan, V.; Puebla-Hellmann, G.; Jung, M.; Hasler, T.; Nunnenkamp, A.; Muoth, M.; Hierold, C.; Wallraff, A.; Schonenberger, C. Clean Carbon Nanotubes Coupled to Superconducting Impedance-Matching Circuits. *Nat. Commun.* **2015**, *6*, 7165.

(4) Penzo, E.; Palma, M.; Wang, R.; Cai, H.; Zheng, M.; Wind, S. J. Directed Assembly of End-Functionalized Single Wall Carbon Nanotube Segments. *Nano Lett.* **2015**, *15*, 6547−6552.

(5) Penzo, E.; Palma, M.; Chenet, D. A.; Ao, G.; Zheng, M.; Hone, J. C.; Wind, S. J. Directed Assembly of Single Wall Carbon Nanotube Field Effect Transistors. *ACS Nano* **2016**, *10*, 2975−2981.

(6) Matsumoto, D.; Yanagi, K.; Takenobu, T.; Okada, S.; Marumoto, K. Electrically Induced Ambipolar Spin Vanishments in Carbon Nanotubes. *Sci. Rep.* **2015**, *5*, 11859.

(7) Wang, H.; Koleilat, G. I.; Liu, P.; Jiménez-Osés, G.; Lai, Y.-C.; Vosgueritchian, M.; Fang, Y.; Park, S.; Houk, K. N.; Bao, Z. High-Yield Sorting of Small-Diameter Carbon Nanotubes for Solar Cells and Transistors. *ACS Nano* **2014**, *8*, 2609−2617.

(8) Marquardt, C. W.; Grunder, S.; Blaszczyk, A.; Dehm, S.; Hennrich, F.; Lohneysen, H. v.; Mayor, M.; Krupke, R. Electroluminescence from a Single Nanotube-Molecule-Nanotube Junction. *Nat. Nanotechnol.* **2010**, *5*, 863−867.

(9) Qi, P.; Vermesh, O.; Grecu, M.; Javey, A.; Wang, Q.; Dai, H.; Peng, S.; Cho, K. J. Toward Large Arrays of Multiplex Functionalized Carbon Nanotube Sensors for Highly Sensitive and Selective Molecular Detection. *Nano Lett.* **2003**, *3*, 347−351.

(10) Kang, Z.; Xu, Y.; Jia, Z. X.; Qin, G. S.; Qin, W. P. 0.8 nm Single Wall Carbon Nanotubes for Wideband Ultrafast Pulse Generation. *Laser Phys.* **2016**, *26*, 045102.

(11) Barone, P. W.; Baik, S.; Heller, D. A.; Strano, M. S. Near-Infrared Optical Sensors Based on Single-Walled Carbon Nanotubes. *Nat. Mater.* **2005**, *4*, 86−92.

(12) Avouris, P.; Chen, Z.; Perebeinos, V. Carbon-based electronics. *Nat. Nanotechnol.* **2007**, *2*, 605−615.

(13) Derycke, V.; Martel, R.; Appenzeller, J.; Avouris, P. Carbon Nanotube Inter- and Intramolecular Logic Gates. *Nano Lett.* **2001**, *1*, 453−456.

(14) Krauss, T. D. Biosensors: Nanotubes light up cells. *Nat. Nanotechnol.* **2009**, *4*, 85−86.

(15) Jain, A.; Homayoun, A.; Bannister, C. W.; Yum, K. Single-Walled Carbon Nanotubes as Near-Infrared Optical Biosensors for Life Sciences and Biomedicine. *Biotechnol. J.* **2015**, *10*, 447−459.

(16) Yang, N.; Chen, X.; Ren, T.; Zhang, P.; Yang, D. Carbon Nanotube Based Biosensors. *Sens. Actuators, B* **2015**, *207*, 690−715.

(17) Fukushima, T.; Kosaka, A.; Ishimura, Y.; Yamamoto, T.; Takigawa, T.; Ishii, N.; Aida, T. Molecular Ordering of Organic Molten Salts Triggered by Single-Walled Carbon Nanotubes. *Science* **2003**, *300*, 2072−2074.

(18) Hirsch, A. Functionalization of Single-Walled Carbon Nanotubes. *Angew. Chem., Int. Ed.* **2002**, *41*, 1853−1859.

(19) Roquelet, C.; Garrot, D.; Lauret, J. S.; Voisin, C.; Alain-Rizzo, V.; Roussignol, P.; Delaire, J. A.; Deleporte, E. Quantum Efficiency of Energy Transfer in Noncovalent Carbon Nanotube/Porphyrin Compounds. *Appl. Phys. Lett.* **2010**, *97*, 141918.

(20) Byrne, M. T.; Gun'ko, Y. K. Recent Advances in Research on Carbon Nanotube-Polymer Composites. *Adv. Mater.* **2010**, *22*, 1672−1688.

(21) Bouilly, D.; Janssen, J. L.; Cabana, J.; Côté, M.; Martel, R. Graft-Induced Midgap States in Functionalized Carbon Nanotubes. *ACS Nano* **2015**, *9*, 2626−2634.

(22) Zhang, J.; Landry, M. P.; Barone, P. W.; Kim, J.-H.; Lin, S.; Ulissi, Z. W.; Lin, D.; Mu, B.; Boghossian, A. A.; Hilmer, A. J.; et al. Molecular Recognition Using Corona Phase Complexes Made of Synthetic Polymers Adsorbed on Carbon Nanotubes. *Nat. Nanotechnol.* **2013**, *8*, 959−968.

(23) Zakaria, A. B.; Picaud, F.; Rattier, T.; Pudlo, M.; Saviot, L.; Chassagnon, R.; Lherminier, J.; Gharbi, T.; Micheau, O.; Herlem, G. Nanovectorization of TRAIL with Single Wall Carbon Nanotubes Enhances Tumor Cell Killing. *Nano Lett.* **2015**, *15*, 891−895.

(24) Prato, M.; Kostarelos, K.; Bianco, A. Functionalized Carbon Nanotubes in Drug Design and Discovery. *Acc. Chem. Res.* **2008**, *41*, 60−68.

(25) Samanta, S. K.; Fritsch, M.; Scherf, U.; Gomulya, W.; Bisri, S. Z.; Loi, M. A. Conjugated Polymer-Assisted Dispersion of Single-Wall Carbon Nanotubes: The Power of Polymer Wrapping. *Acc. Chem. Res.* **2014**, *47*, 2446−2456.

(26) Hasan, T.; Sun, Z.; Tan, P.; Popa, D.; Flahaut, E.; Kelleher, E. J. R.; Bonaccorso, F.; Wang, F.; Jiang, Z.; Torrisi, F.; et al. Double-Wall Carbon Nanotubes for Wide-Band, Ultrafast Pulse Generation. *ACS Nano* **2014**, *8*, 4836−4847.

(27) Welsher, K.; Liu, Z.; Sherlock, S. P.; Robinson, J. T.; Chen, Z.; Daranciang, D.; Dai, H. A Route to Brightly Fluorescent Carbon

Nanotubes for Near-Infrared Imaging in Mice. *Nat. Nanotechnol.* **2009**, *4*, 773−780.
(28) Hong, G.; Diao, S.; Antaris, A. L.; Dai, H. Carbon Nanomaterials for Biological Imaging and Nanomedicinal Therapy. *Chem. Rev.* **2015**, *115*, 10816−10906.
(29) Kong, J.; Franklin, N. R.; Zhou, C.; Chapline, M. G.; Peng, S.; Cho, K.; Dai, H. Nanotube Molecular Wires as Chemical Sensors. *Science* **2000**, *287*, 622−625.
(30) Chen, R. J.; Bangsaruntip, S.; Drouvalakis, K. A.; Wong Shi Kam, N.; Shim, M.; Li, Y.; Kim, W.; Utz, P. J.; Dai, H. Noncovalent Functionalization of Carbon Nanotubes for Highly Specific Electronic Biosensors. *Proc. Natl. Acad. Sci. U. S. A.* **2003**, *100*, 4984−4989.
(31) Hersam, M. C. Progress towards monodisperse single-walled carbon nanotubes. *Nat. Nanotechnol.* **2008**, *3*, 387−394.
(32) Zhang, T.; Nix, M. B.; Yoo, B.-Y.; Deshusses, M. A.; Myung, N. V. Electrochemically Functionalized Single-Walled Carbon Nanotube Gas Sensor. *Electroanalysis* **2006**, *18*, 1153−1158.
(33) Zhang, T.; Mubeen, S.; Yoo, B.; Myung, N. V.; Deshusses, M. A. A Gas Nanosensor Unaffected by Humidity. *Nanotechnology* **2009**, *20*, 255501.
(34) Shirsat, M. D.; Sarkar, T.; Kakoullis, J., Jr; Myung, N. V.; Konnanath, B.; Spanias, A.; Mulchandani, A. Porphyrin-Functionalized Single-Walled Carbon Nanotube Chemiresistive Sensor Arrays for VOCs. *J. Phys. Chem. C* **2012**, *116*, 3845−3850.
(35) Rushi, A.; Datta, K.; Ghosh, P.; Mulchandani, A.; Shirsat, M. Iron Tetraphenyl Porphyrin Functionalized Single Wall Carbon Nanotubes for the Detection of Benzene. *Mater. Lett.* **2013**, *96*, 38−41.
(36) Hill, D.; Lin, Y.; Qu, L.; Kitaygorodskiy, A.; Connell, J. W.; Allard, L. F.; Sun, Y.-P. Functionalization of Carbon Nanotubes with Derivatized Polyimide. *Macromolecules* **2005**, *38*, 7670−7675.
(37) Stevens, J. L.; Huang, A. Y.; Peng, H.; Chiang, I. W.; Khabashesku, V. N.; Margrave, J. L. Sidewall Amino-Functionalization of Single-Walled Carbon Nanotubes through Fluorination and Subsequent Reactions with Terminal Diamines. *Nano Lett.* **2003**, *3*, 331−336.
(38) Clavé, G.; Delport, G.; Roquelet, C.; Lauret, J.-S.; Deleporte, E.; Vialla, F.; Langlois, B.; Parret, R.; Voisin, C.; Roussignol, P.; et al. Functionalization of Carbon Nanotubes through Polymerization in Micelles: A Bridge between the Covalent and Noncovalent Methods. *Chem. Mater.* **2013**, *25*, 2700−2707.
(39) Yarotski, D. A.; Kilina, S. V.; Talin, A. A.; Tretiak, S.; Prezhdo, O. V.; Balatsky, A. V.; Taylor, A. J. Scanning Tunneling Microscopy of DNA-Wrapped Carbon Nanotubes. *Nano Lett.* **2009**, *9*, 12−17.
(40) Shim, M.; Kam, N. W. S.; Chen, R. J.; Li, Y.; Dai, H. Functionalization of Carbon Nanotubes for Biocompatibility and Biomolecular Recognition. *Nano Lett.* **2002**, *2*, 285−288.
(41) Worsley, K. A.; Moonoosawmy, K. R.; Kruse, P. Long-Range Periodicity in Carbon Nanotube Sidewall Functionalization. *Nano Lett.* **2004**, *4*, 1541−1546.
(42) Bonifazi, D.; Nacci, C.; Marega, R.; Campidelli, S.; Ceballos, G.; Modesti, S.; Meneghetti, M.; Prato, M. Microscopic and Spectroscopic Characterization of Paintbrush-like Single-walled Carbon Nanotubes. *Nano Lett.* **2006**, *6*, 1408−1414.
(43) Nemes-Incze, P.; Kónya, Z.; Kiricsi, I.; Pekker, A.; Horváth, Z. E.; Kamarás, K.; Biró, L. P. Mapping of Functionalized Regions on Carbon Nanotubes by Scanning Tunneling Microscopy. *J. Phys. Chem. C* **2011**, *115*, 3229−3235.
(44) Sáfar, G. d. A. M.; da Silva Martins, D. C.; DeFreitas-Silva, G.; Rebouças, J. S.; Idemori, Y. M.; Righi, A. Interactions of porphyrins and single walled carbon nanotubes: A fine duet. *Synth. Met.* **2014**, *193*, 64−70.
(45) Roquelet, C.; Lauret, J.-S.; Alain-Rizzo, V.; Voisin, C.; Fleurier, R.; Delarue, M.; Garrot, D.; Loiseau, A.; Roussignol, P.; Delaire, J. A.; et al. π-Stacking Functionalization of Carbon Nanotubes through Micelle Swelling. *ChemPhysChem* **2010**, *11*, 1667−1672.
(46) Delport, G.; Orcin-Chaix, L.; Campidelli, S.; Voisin, C.; Lauret, J.-S. Controlling the Kinetics of the Non-Covalent Functionalization of Carbon Nanotubes Using sub-cmc Dilutions in a Co-Surfactant Environment. *Nanoscale* **2017**, *9*, 2646−2651.
(47) Vialla, F.; Delport, G.; Chassagneux, Y.; Roussignol, P.; Lauret, J.-S.; Voisin, C. Diameter-Selective Non-Covalent Functionalization of Carbon Nanotubes With Porphyrin Monomers. *Nanoscale* **2016**, *8*, 2326−2332.
(48) Vialla, F.; Roquelet, C.; Langlois, B.; Delport, G.; Santos, S. M.; Deleporte, E.; Roussignol, P.; Delalande, C.; Voisin, C.; Lauret, J.-S. Chirality Dependence of the Absorption Cross Section of Carbon Nanotubes. *Phys. Rev. Lett.* **2013**, *111*, 137402.
(49) Sun, H. COMPASS: An ab Initio Force-Field Optimized for Condensed-Phase Applications Overview with Details on Alkane and Benzene Compounds. *J. Phys. Chem. B* **1998**, *102*, 7338−7364.
(50) *Materials Studio Release Notes*, Release 7.0; Accelrys Software Inc.: San Diego, CA., USA., 2013.
(51) Odom, T. W.; Huang, J.-L.; Kim, P.; Lieber, C. M. Atomic Structure and Electronic Properties of Single-Walled Carbon Nanotubes. *Nature* **1998**, *391*, 62−64.
(52) Wilder, J. W. G.; Venema, L. C.; Rinzler, A. G.; Smalley, R. E.; Dekker, C. Electronic Structure of Atomically Resolved Carbon Nanotubes. *Nature* **1998**, *391*, 59−62.
(53) Venema, L. C.; Meunier, V.; Lambin, P.; Dekker, C. Atomic Structure of Carbon Nanotubes from Scanning Tunneling Microscopy. *Phys. Rev. B: Condens. Matter Mater. Phys.* **2000**, *61*, 2991−2996.
(54) Pham, V. D.; Lagoute, J.; Mouhoub, O.; Joucken, F.; Repain, V.; Chacon, C.; Bellec, A.; Girard, Y.; Rousset, S. Electronic Interaction Between Nitrogen-Doped Graphene and Porphyrin Molecules. *ACS Nano* **2014**, *8*, 9403−9409.
(55) Bussetti, G.; Campione, M.; Riva, M.; Picone, A.; Raimondo, L.; Ferraro, L.; Hogan, C.; Palummo, M.; Brambilla, A.; Finazzi, M.; et al. Stable Alignment of Tautomers at Room Temperature in Porphyrin 2D Layers. *Adv. Funct. Mater.* **2014**, *24*, 958−963.
(56) Kim, H.; Chang, Y. H.; Lee, S.-H.; Kim, Y.-H.; Kahng, S.-J. Switching and Sensing Spin States of Co-Porphyrin in Bimolecular Reactions on Au(111) Using Scanning Tunneling Microscopy. *ACS Nano* **2013**, *7*, 9312−9317.
(57) Wang, W.; Pang, R.; Kuang, G.; Shi, X.; Shang, X.; Liu, P. N.; Lin, N. Intramolecularly Resolved Kondo Resonance of High-Spin Fe(II)-Porphyrin Adsorbed on Au(111). *Phys. Rev. B: Condens. Matter Mater. Phys.* **2015**, *91*, 045440.
(58) Xu, J.; Mueller, R.; Hazelbaker, E.; Zhao, Y.; Bonzongo, J.-C. J.; Clar, J. G.; Vasenkov, S.; Ziegler, K. J. Strongly Bound Sodium Dodecyl Sulfate Surrounding Single-Wall Carbon Nanotubes. *Langmuir* **2017**, *33*, 5006−5014.
(59) Richard, C.; Balavoine, F.; Schultz, P.; Ebbesen, T. W.; Mioskowski, C. Supramolecular Self-Assembly of Lipid Derivatives on Carbon Nanotubes. *Science* **2003**, *300*, 775−778.
(60) Ilan, B.; Florio, G. M.; Hybertsen, M. S.; Berne, B. J.; Flynn, G. W. Scanning Tunneling Microscopy Images of Alkane Derivatives on Graphite: Role of Electronic Effects. *Nano Lett.* **2008**, *8*, 3160−3165.
(61) Yin, X.-L.; Wan, L.-J.; Yang, Z.-Y.; Yu, J.-Y. Self-Organization of Surfactant Molecules on Solid Surface: an STM Study of Sodium Alkyl Sulfonates. *Appl. Surf. Sci.* **2005**, *240*, 13−18.
(62) Zhao, M.; Jiang, P.; Deng, K.; Yu, A.-F.; Hao, Y.-Z.; Xie, S.-S.; Sun, J.-L. Insight into STM Image Contrast of n-Tetradecane and n-Hexadecane Molecules on Highly Oriented Pyrolytic Graphite. *Appl. Surf. Sci.* **2011**, *257*, 3243−3247.
(63) Xu, S.-L.; Wang, C.; Zeng, Q.-D.; Wu, P.; Wang, Z.-G.; Yan, H.-K.; Bai, C.-L. Self-Assembly of Cationic Surfactants on a Graphite Surface Studied by STM. *Langmuir* **2002**, *18*, 657−660.
(64) Endo, O.; Horikoshi, T.; Katsumata, N.; Otani, K.; Fujishima, T.; Goto, H.; Minami, K.; Akaike, K.; Ozaki, H.; Sumii, R.; et al. Incommensurate Crystalline Phase of n-Alkane Monolayers on Graphite (0001). *J. Phys. Chem. C* **2011**, *115*, 5720−5725.
(65) Herwig, K. W.; Matthies, B.; Taub, H. Solvent Effects on the Monolayer Structure of Long n-Alkane Molecules Adsorbed on Graphite. *Phys. Rev. Lett.* **1995**, *75*, 3154−3157.
(66) Florio, G. M.; Ilan, B.; Müller, T.; Baker, T. A.; Rothman, A.; Werblowsky, T. L.; Berne, B. J.; Flynn, G. W. Solvent Effects on the Self-Assembly of 1-Bromoeicosane on Graphite. Part I. Scanning Tunneling Microscopy. *J. Phys. Chem. C* **2009**, *113*, 3631−3640.

DOI: 10.1021/acs.jpcc.7b06890
J. Phys. Chem. C 2017, 121, 24264−24271